Manganese Complexes of 1,3-Bis(3-nitrosalicylideneamino)-propan-2-ol. Structure and Magnetic and Electrochemical Properties†

Zhi-Yong Zhang, Chantal Brouca-Cabarrecq, Catherine Hemmert, Françoise Dahan and Jean-Pierre Tuchagues*

Laboratoire de Chimie de Coordination du CNRS, UPR 8241 liée par conventions à l'Université Paul Sabatier et à l'Institut National Polytechnique, 205 route de Narbonne, 31077 Toulouse Cedex, France

Four complexes [Mn$^{\text{II}}$(3NO$_2$-Hsalpro)] **1**, [Mn$^{\text{II}}_2$(3NO$_2$-salpro)(O$_2$CMe)]·4MeOH **2**, [Mn$^{\text{III}}_2$(3NO$_2$-salpro)$_2$(H$_2$O)]·H$_2$O **3** and [{Mn$^{\text{III}}$(3NO$_2$-salpro)}$_2$]·2dmf **4**, [3NO$_2$-H$_3$salpro = 1,3-bis(3-nitrosalicylideneamino)propan-2-ol, dmf = dimethylformamide] have been synthesized and studied. The structure of **4** was solved by direct methods and refined to conventional agreement indices $R = R' = 0.041$. The molecular structure consists of discrete [{Mn$^{\text{III}}$(3NO$_2$-salpro)}$_2$] units and lattice-held dmf molecules. The co-ordination octahedron around each Mn$^{\text{III}}$ includes three donors from each of the two pentadentate trianionic ligands. Both ligands asymmetrically bridge the Mn atoms affording an intra-dinuclear Mn···Mn' separation of 3.223(1) Å. The symmetry-related manganese centres are in a distorted-octahedral environment. Infrared, ESR spectroscopic, magnetic susceptibility and electrochemical studies of **1**–**4** evidence a variety of structural types and nuclearities. Complex **1**, resulting from the reaction of manganese(II) acetate with 3NO$_2$-H$_3$salpro, is characterized by the MnL stoichiometry while **2**, resulting from the reaction of manganese(II) acetate with Na$_3$(3NO$_2$-salpro), is characterized by the Mn$_2$L stoichiometry. Two structurally different dinuclear manganese(III) complexes characterized by the same overall formulation [{Mn$^{\text{III}}$(3NO$_2$-salpro)(solvent)}$_2$] were obtained from the reaction of **1** with O$_2$. In non-dehydrated methanol, the asymmetric dinuclear species **3** is formed. When this complex is dissolved in dry dmf the water molecule is driven out of the manganese co-ordination sphere and a subsequent ligand environment reorganization affords **4**. Variable-temperature magnetic susceptibility studies established the presence of isotropic magnetic exchange interactions between the manganese(III) centres of the dimeric species **3** and **4** ($J = -1.9$ and -1.6 cm^{-1}, respectively) and crystalline field anisotropy of Mn$^{\text{III}}$ ($D = -2.6$ and -2.5 cm^{-1}, respectively). Electrochemical studies indicated that the Mn$^{\text{II}}_2$, Mn$^{\text{II}}$Mn$^{\text{III}}$, Mn$^{\text{III}}_2$ and Mn$^{\text{III}}$Mn$^{\text{IV}}$ oxidation states are accessible for **4** in dmf–water.

The potentially pentadentate 1,3-bis(X-substituted salicylideneamino)propan-2-ol (X = H, 3-MeO, 5-Cl, 5-Br, 5-NO$_2$, 3,5-Cl$_2$), abbreviated X-H$_3$salpro throughout this report, has been extensively used in the co-ordination chemistry of transition-metal ions due to its ability to afford a variety of co-ordination modes related to the nature of the ONONO donor set and the versatile accessibility of the dianionic Hsalpro or trianionic salpro forms.

In the first reported metal complex including the generic H$_3$salpro ligand (X = H) a terdentate co-ordination to tin(IV) was postulated.[1] A similar mode has recently been proposed in the case of dioxomolybdenum(VI) complexes of Hsalpro and related ligands.[2] Tetradentate co-ordination of Hsalpro has been observed for mononuclear copper and manganese compounds,[3–5] manganese chains[4,5] and technetium and rhenium mono- or di-nuclear oxo-complexes.[6] Zelentsov *et al.*[7] have postulated the involvement of all five atoms of the N$_2$O$_3$ donor set in the co-ordination of X-salpro (X = H, 3-MeO, 5-Cl, 5-Br or 5-NO$_2$) to manganese(III) and dimerization of the resulting Mn$^{\text{III}}$(X-salpro) molecules through two phenolate oxygen donors, each pertaining to one of the molecules. Similarly, a dimeric structure has been postulated for Fe$^{\text{III}}$(salpro)·(0.5thf)[8] (thf = tetrahydrofuran) and Fe$^{\text{III}}$(salpro)[9] and dimeric or oligomeric structures suggested for Fe$^{\text{II}}$(Hsalpro), Fe$^{\text{II}}$(Hsalpro)(acac) (acac = acetylacetonate) and Mn$^{\text{II}}$(Hsalpro).[8,10]

The dinucleating ability of such ligands has been widely illustrated with copper, nickel, iron and oxovanadium complexes of the M$_2$(salpro)X type.[3,5,9,11–17] In all these complexes the central alcoholate oxygen atom of the salpro trianion acts as a symmetric endogenous bridge and both metal centres are equivalently chelated by one phenolate oxygen, one imine nitrogen and the central alcoholate oxygen donors of the pentadentate ligand. The resulting dinuclear structure is stabilized by an exogenous bridging anion (OH, OMe, MeCO$_2$ or pyrazolate). Surprisingly, this type of dinuclear structure has not yet been evidenced in the case of manganese despite the extensive work carried out by several groups in view of the biological importance of dinuclear manganese compounds as models of manganese enzymes.[18–20]

However, the renewed interest in the reaction of manganese with this type of compound has recently provided several new types of dinuclear manganese compounds. An asymmetric [Mn$^{\text{III}}_2$(X-salpro)$_2$(O$_{\text{solvent}}$)] structure (solvent = MeOH,[4] thf[5] or water[21]) in which each trianionic ligand distributes differently its five donor atoms between the two manganese centres has been characterized by X-ray diffraction. While one of the salpro trianions acts as a bridging ligand through its central alcoholate oxygen donor, the second acts as a tridentate ONO chelate for one of the manganese(III) cations and a

---

† *Supplementary data available* (No SUP 57076, 6 pp.): IR data for the isolated ligand and complexes 1–4; and complete magnetic susceptibility data. See Instructions for Authors, *J. Chem. Soc., Dalton Trans.*, 1995, Issue 1, pp. xxv–xxx.

Non-SI unit employed: $\mu_B \approx 9.27 \times 10^{-24}$ J T^{-1}.

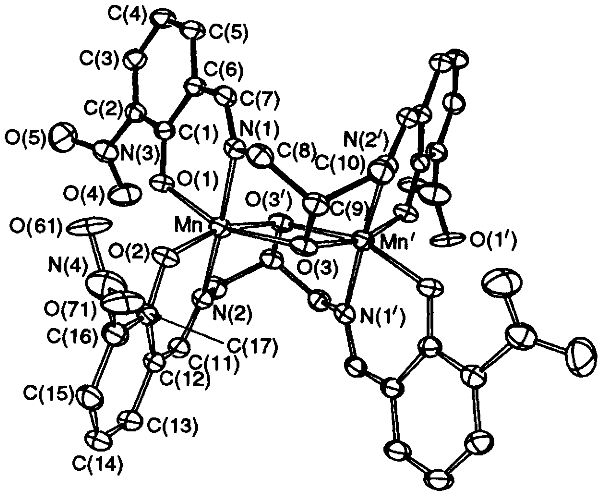

Fig. 1 An ORTEP[25] view of the dinuclear complex molecule $[\{Mn^{III}(3NO_2\text{-salpro})\}_2]$ **4** with atom labelling. The hydrogen atoms are omitted for clarity

bidentate NO chelate for the other. The free co-ordination site left on one manganese by this peculiar ligand distribution is occupied by the oxygen donor of the solvent molecule. A similar asymmetric structure has been found for the mixed-valence $[Mn^{IV}(3,5Cl_2\text{-salpro})_2Mn^{III}(thf)]ClO_4$.[22] More recently, a dinuclear symmetric structure has been reported in which both $5NO_2$-salpro trianions act as bridging ligands through their central alcoholate oxygen donor and distribute equivalently their five donor atoms between the two manganese(III) centres.[23] Finally, in $[(Mn^{III}L)_2]\cdot 2MeCN$,[24] where H_3L (1-salicylamino-3-salicylideneaminopropan-2-ol) results from the reduction of one imine function of H_3salpro, each Mn^{III} is co-ordinated to the five donor atoms of one trianionic ligand and the resulting $Mn^{III}L$ molecules are associated in pairs through oxygen bridges afforded by the central alcoholate oxygen function of each ligand.

The amazing co-ordination versatility of the X-H_3salpro ligands and the biological importance of binuclear manganese compounds as models of manganese enzymes prompted us to study further their co-ordination chemistry with manganese. In this contribution we describe four distinct structural types for manganese complexes of 1,3-bis(3-nitrosalicylideneamino)-propan-2-ol ($3NO_2$-H_3salpro) and report their magnetic and electrochemical behaviour.

Results and Discussion

Compositional Studies.—The analytical results evidence that the reaction of $3NO_2$-H_3salpro with manganese(II) acetate tetrahydrate under anaerobic conditions leads to two distinct manganese(II) complexes. When stoichiometric amounts of $3NO_2$-H_3salpro and manganese salt are allowed to react an orange solid formulated as $[Mn^{II}(3NO_2\text{-Hsalpro})]$ **1** is obtained, while the reaction of 1 equivalent of $3NO_2$-H_3salpro with 3 equivalents of Na(OEt) and 2 equivalents of $Mn(O_2CMe)_2$ yields an orange solid $[Mn^{II}_2(3\text{-}NO_2\text{-salpro})(O_2CMe)]\cdot 4MeOH$ **2**. Oxidation of **2** with dioxygen did not afford any definite species. On the contrary, the reaction of methanolic solutions of **1** with dioxygen yields dark brown microcrystals of $[Mn^{III}_2(3NO_2\text{-salpro})_2(H_2O)]\cdot H_2O$ **3**. While crystals of **3** suitable for X-ray analysis could not be obtained by recrystallization from methanol, dark brown single crystals of $[\{Mn^{III}(3NO_2\text{-salpro})\}_2]\cdot 2dmf$ **4** (dmf = dimethylformamide) were obtained by slow concentration of dmf–toluene solutions of **3**.

Table 1 Final fractional atomic coordinates for $[\{Mn^{III}(3NO_2\text{-salpro})\}_2]\cdot 2dmf$ **4**

Atom	*x*	*y*	*z*
Mn	0.413 76(6)	0.406 57(5)	−0.000 36(6)
O(1)	0.236 4(2)	0.409 2(2)	−0.114 1(3)
O(2)	0.444 8(3)	0.267 3(2)	0.128 5(3)
O(3)	0.562 6(2)	0.474 0(2)	0.133 8(2)
N(1)	0.311 9(3)	0.529 4(3)	0.128 9(3)
N(2)	0.505 0(3)	0.282 2(3)	−0.130 5(3)
C(1)	0.128 5(3)	0.502 8(3)	−0.129 0(4)
C(2)	0.023 7(4)	0.508 7(3)	−0.242 2(4)
C(3)	−0.096 7(4)	0.602 2(4)	−0.256 2(4)
C(4)	−0.118 3(4)	0.697 4(4)	−0.158 4(5)
C(5)	−0.020 5(4)	0.696 6(4)	−0.046 8(5)
C(6)	0.102 5(4)	0.602 9(3)	−0.029 1(4)
C(7)	0.193 4(4)	0.603 9(3)	0.098 5(4)
C(8)	0.388 6(4)	0.524 1(4)	0.270 4(4)
C(9)	0.525 7(4)	0.528 8(3)	0.262 3(4)
C(10)	0.532 4(4)	0.663 8(4)	0.272 3(4)
C(11)	0.579 7(4)	0.167 7(3)	−0.104 4(4)
C(12)	0.604 2(3)	0.102 9(3)	0.026 9(4)
C(13)	0.691 5(4)	−0.020 4(4)	0.041 4(5)
C(14)	0.713 9(4)	−0.092 2(4)	0.158 6(5)
C(15)	0.649 1(4)	−0.042 6(4)	0.266 8(5)
C(16)	0.561 3(4)	0.078 7(4)	0.254 4(4)
C(17)	0.533 2(3)	0.156 3(3)	0.136 0(4)
N(3)	0.038 3(4)	0.409 4(3)	−0.347 6(4)
O(4)	0.141 0(4)	0.368 6(4)	−0.390 5(4)
O(5)	−0.054 9(4)	0.372 8(4)	−0.392 7(5)
N(4)	0.497 6(5)	0.126 8(5)	0.371 3(5)
O(61)	0.385 0(6)	0.185 9(18)	0.379 5(12)
O(71)	0.566 9(9)	0.116 3(12)	0.487 2(7)
O(62)	0.413 5(9)	0.079 5(8)	0.380 4(10)
O(72)	0.497 3(15)	0.229 9(7)	0.418 5(9)
N(5)	0.999 3(4)	−0.086 3(4)	0.697 3(4)
C(18)	0.896 6(5)	−0.079 0(5)	0.577 0(5)
C(19)	1.122 4(5)	−0.186 9(5)	0.695 8(6)
C(20)	0.979 8(7)	−0.012 1(6)	0.808 0(6)
O(8)	0.877 3(5)	0.071 5(5)	0.818 2(6)

Table 2 Selected interatomic distances (Å) and angles (°) with estimated standard deviations (e.s.d.s) in parentheses for $[\{Mn^{III}(3NO_2\text{-salpro})\}_2]\cdot 2dmf$ **4**

Mn–O(1)	2.032(2)	Mn–O(3′)	2.006(3)
Mn–O(2)	1.944(3)	Mn–N(1)	2.012(3)
Mn–O(3)	2.183(3)	Mn–N(2)	1.977(3)
Mn ··· Mn	3.223(1)		
Mn–O(3)–Mn′	100.51(9)	O(2)–Mn–N(1)	90.9(1)
O(1)–Mn–O(2)	99.8(1)	O(2)–Mn–N(2)	88.2(1)
O(1)–Mn–O(3)	159.25(8)	O(3)–Mn–O(3′)	79.49(9)
O(1)–Mn–O(3′)	93.0(1)	O(3)–Mn–N(1)	76.5(1)
O(1)–Mn–N(1)	86.1(1)	O(3)–Mn–N(2)	106.7(1)
O(1)–Mn–N(2)	90.9(1)	O(3′)–Mn–N(2)	100.8(1)
O(2)–Mn–O(3)	91.8(1)	O(3′)–Mn–N(2)	80.7(1)
O(2)–Mn–O(3′)	163.3(1)	N(1)–Mn–N(2)	176.7(1)

Primed atoms are related by the symmetry operation 1 − *x*, 1 − *y*, −*z*.

Crystal and Molecular Structure of $[\{Mn^{III}(3NO_2\text{-salpro})\}_2]\cdot 2dmf$ **4**.—A thermal ellipsoid drawing of the structure for the dinuclear unit of complex **4** including the atom numbering scheme is depicted in Fig. 1. The crystallographic data are in the Experimental section. Final fractional atomic coordinates with their estimated standard deviations and selected bond distances and angles appear in Tables 1 and 2 respectively.

The molecular structure consists of discrete $[\{Mn^{III}(3NO_2\text{-salpro})\}_2]$ units and lattice-held dmf molecules. The co-ordination octahedron around each Mn^{III} includes three donors from each of the two pentadentate trianionic ligands: Mn is co-ordinated to O(1), N(1) and O(3) from L^1 and O(2), N(2) and O(3′) from L^2, Mn′ to O(2′), N(2′) and O(3) from L^1 and O(1′), N(1′) and O(3′) from L^2. Both ligands asymmetrically bridge

Mn to Mn' through the alcoholate oxygen atoms O(3) and O(3') affording an intra-dinuclear Mn • • • Mn' separation of 3.223(1) Å.

The symmetry-related Mn and Mn' cations are in a distorted-octahedral environment: the O(1) phenolate and O(3) alcoholate oxygen atoms are situated at the apices of the distorted octahedron around Mn while its equatorial plane includes the phenolate O(2) and alcoholate O(3') oxygen and imine nitrogen atoms N(1) and N(2). Since axial Mn–L bond distances are longer than the four equatorial ones, the main distortion of the co-ordination octahedron is an axial elongation along O(1) • • • O(3). An examination of the dihedral angles between the octahedron faces and their departure from equilaterality and the angles between the co-ordination planes substantiates that the axial elongation along O(1) • • • O(3) is the main distortion. However, it also reveals other distortions which lower even more the symmetry of the ligand environment. For example, the asymmetric alcoholate bridge between Mn and Mn' decreases the O(3)–Mn–N(1) and O(3)–Mn–O(3') angles to 76.5(1) and 79.49(9)°, respectively.

The crystal packing results from aromatic ring stackings between the salicylaldimine parts of the 3NO$_2$-salpro ligands from dinuclear molecules related through the symmetries $-x$, $1-y$, $-z$ ('') and $1-x$, $-y$, $-z$ ('''). Dimethylformamide molecules are inserted between all adjacent dinuclear units. The shortest inter-dinuclear distances between manganese cations are Mn • • • Mn'' 8.616(1) and Mn • • • Mn''' 8.651(1) Å.

Infrared Spectroscopy.—The IR spectra are consistent with the compositional differences suggested by the analytical results as complex **2** exhibits ν_{asym} and ν_{sym} frequencies characteristic of the acetate anion while **1**, **3** and **4** do not. The Δ value ($\nu_{asym} - \nu_{sym}$) of 130 cm^{-1} indicates that the acetate anion of **2** bridges the two manganese(II) cations.[26] The very strong and broad O–H absorption located between 3400 and 3280 cm^{-1} (associated with the stretching of the terminal phenolic and central alcoholic functions of the isolated ligand) is replaced by a weak absorption at 3372 cm^{-1} in the IR spectrum of **1** (central alcoholic function of the co-ordinated ligand) and 3400 cm^{-1} in that of **2** (co-ordinated methanol) and two absorptions (3540 and 3424 cm^{-1}) in the spectrum of **3** (which probably arise respectively from the unco-ordinated and co-ordinated water molecules). The absorption for **4** at 1660 cm^{-1} is characteristic of the formation of a dmf solvate. The shift in C=N imine absorption wavenumber between the isolated ligand and complexes (−20 to −34 cm^{-1}) clearly indicates the co-ordination of the imine nitrogen atoms to the manganese in all four complexes. Similarly, the absorptions attributable to the NO$_2$ substituents are slightly shifted upon complexation. The C–O absorption for the central alcoholic function of the ligand is observed at 1040 cm^{-1} (CHOH) for the isolated ligand, 1048 cm^{-1} (CHOH) for **1**, 1045 cm^{-1} (CHO$^-$) for **2** and 1041 cm^{-1} (CHO$^-$) for **3** and **4**. The observation of a second C–O absorption (1032 cm^{-1}) in the IR spectrum of **2** confirms the presence of co-ordinated methanol. We tentatively assign the low-frequency absorptions observed in the spectra of complexes **1**–**4** and lacking in the ligand spectrum to Mn–L vibration modes, some of them being probably coupled to ligand vibrations.[27,28]

ESR Spectroscopy and Magnetic Susceptibility.—As expected, the manganese(II) complexes **1** and **2** are the only ESR-active species in this series. Their X-band powder spectra exhibit a temperature-independent (300–80 K) and featureless broad resonance with $g \approx 2.0$. The broadness of these isotropic signals is consistent with a polymeric manganese(II) structure in the solid state for both compounds.[10,29] While the X-band frozen-solution spectrum (dmf–toluene, 1 : 1) of complex **2** is similar to its powder spectrum, the glass spectrum of **1** exhibits several fine-structure resonances spread out over 6000 G (0.6 T), some of them being further split into the characteristic ^{55}Mn six-line pattern. It is thus clear that while the inter-dinuclear associations of [Mn$^{II}_2$(3NO$_2$-salpro)(O$_2$CMe)]•4MeOH **2** are retained in solution, the solid-state polymeric structure of **1** dissociates into mononuclear [Mn^{II}(3NO$_2$-Hsalpro)] species in the dmf–toluene solvent mixture.

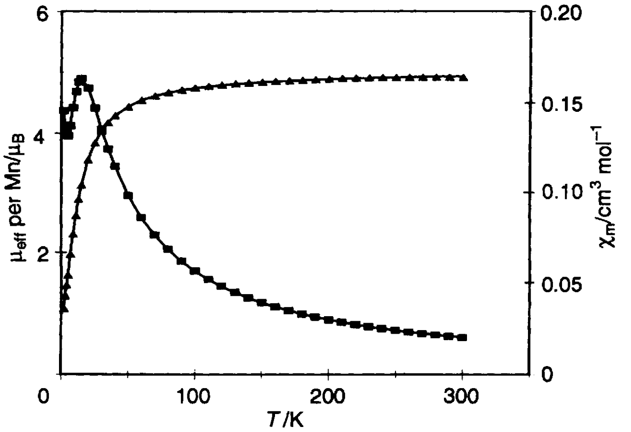

Fig. 2 Variable-temperature magnetic susceptibility data for [Mn$^{III}_2$(3NO$_2$-salpro)$_2$(H$_2$O)]•H$_2$O **3**. The solid lines result from a least-squares fit of the data to the theoretical magnetic susceptibility calculated by exact diagonalization of the effective spin Hamiltonian taking into account single-ion zero-field splitting

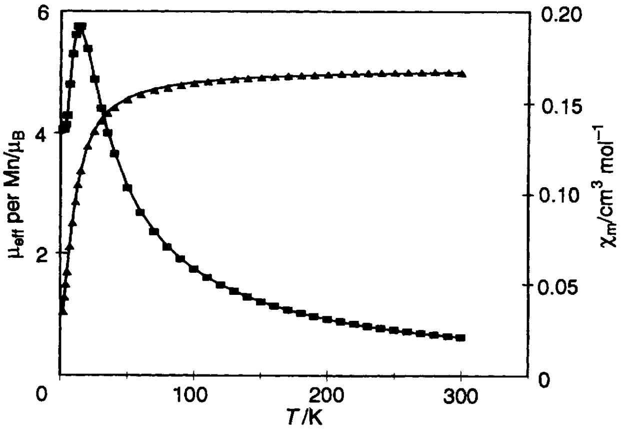

Fig. 3 Variable-temperature magnetic susceptibility data for [{Mn^{III}(3NO$_2$-salpro)}$_2$]•2dmf **4**. Details as in Fig. 2

The effective magnetic moment per manganese at selected temperatures is reported in Table 3 for complexes **1**–**4** and the detailed data resulting from the magnetic susceptibility measurements are available as SUP 57076. The effective magnetic moment per manganese(II) ion increases appreciably as the temperature is decreased below *ca.* 50 K and reaches a maximum of 6.5 μ_B at 5 K for complex **1**, indicating that a weak ferromagnetic exchange interaction is present in this polymeric compound. On the other hand, μ_{eff} for **2** decreases appreciably as the temperature is decreased below *ca.* 100 K and reaches 1.8 μ_B at 2 K, indicating that antiferromagnetic exchange interactions are operating in this polymeric association of dinuclear units. In view of the lack of structural information, the magnetic behaviour of **1** and **2** was not further investigated.

The temperature dependence of the magnetic susceptibility and effective magnetic moment per manganese of the manganese(III) dinuclear complexes **3** and **4** are shown in Figs. 2 and 3, respectively: μ_{eff} per Mn decreases from 4.91 and 4.99 μ_B at 300 K to 1.08 and 1.04 μ_B at 2 K for **3** and **4**, respectively, indicating a weak antiferromagnetic coupling of the $S = 2$ spin systems of the two manganese(III) ions of each dinuclear complex.

We have thus initially analysed the variation of the magnetic

Table 3 Magnetic moment per manganese at selected temperatures for complexes **1–4**

	μ_{eff}/μ_B				
Complex	300	100	50	20	2 K
1 $[Mn^{III}(3NO_2\text{-}Hsalpro)]$	5.60	5.68	5.75	5.97	5.53
2 $[Mn^{III}_2(3NO_2\text{-}salpro)(O_2CMe)]\cdot 4MeOH$	5.51	5.03	4.45	3.51	1.77
3 $[Mn^{III}_2(3NO_2\text{-}salpro)_2(H_2O)]\cdot H_2O$	4.91	4.75	4.44	3.56	1.08
4 $[\{Mn^{III}(3NO_2\text{-}salpro)\}_2]\cdot 2dmf$	4.99	4.82	4.55	3.79	1.04

susceptibility of complexes **3** and **4** by employing the expression derived from the isotropic spin-exchange Hamiltonian $\mathscr{H} = -2JS_1S_2$ ($S_1 = S_2 = 2$) and the van Vleck equation.[30] Although the least-squares refinements obtained with this model afforded a reasonable fit for $J \approx -2$ cm^{-1} in the high-temperature range, the fit was poor below 40 K for both compounds. When the above equation was modified to take into account interdimer interactions in the molecular field approximation[31] it afforded poorer results. The inability of the two methods to account for the experimental results indicates that the antiferromagnetic behaviour of **3** and **4** cannot be interpreted by considering only isotropic exchange interactions. Since the experimental results suggested that the magnetic exchange interactions in **3** and **4** are weak, the crystalline field anisotropy and the magnetic exchange interactions are expected to be of the same order of magnitude. Consequently, we attempted to fit the experimental data by the theoretical magnetic susceptibility calculated by exact diagonalization of the effective spin Hamiltonian taking into account single-ion zero-field splitting (z.f.s.).[32] The least-squares refinements calculated from this model afforded very good fits (Figs. 2 and 3) for the parameters: **3**, $J = -1.9$ cm^{-1}, $D = -2.6$ cm^{-1}, $g_\perp = 2.006$, $g_\parallel = 2.076$, $P = 2\%$; **4**, $J = -1.6$ cm^{-1}, $D = -2.5$ cm^{-1}, $g_\perp = 2.041$, $g_\parallel = 2.098$ and $P = 0.6\%$; where P is the mole percent of a paramagnetic impurity assumed to be a manganese(III) monomer. The absolute values obtained for D clearly indicate that the magnetic behaviour of **3** and **4** is such that the z.f.s. of the single ion is of the order of magnitude of the exchange integral and cannot be treated as a perturbation. The fact that reasonable fits could only be obtained for negative D values indicates that the axial distortion of the ligand environment of the manganese must be an elongation. In this regard it is interesting that the distortion observed for the co-ordination octahedron of the manganese in the complexes $[Mn^{III}_2(5Cl\text{-}salpro)_2(MeOH)]$,[4] $[Mn^{III}_2(salpro)_2(thf)]$[5] and $[Mn^{III}_2(salpro)_2(H_2O)]\cdot 3MeOH$[21] structurally related to **3** is an axial elongation. Similarly, the symmetry-related Mn and Mn′ cations of the dinuclear $[\{Mn^{III}(3NO_2\text{-}salpro)\}_2]$ unit of **4** are in a distorted-octahedral environment with O(1) and O(3) situated at the apices of the distorted octahedron. Since both axial Mn–L bond lengths are larger than the four equatorial ones, the structural evidence for axial elongation indicates a $^5B_{1g}$ ground state (D is negative).

The most significant parameters resulting from the analysis of the magnetic and structural properties of complexes **3** and **4**, together with those of eight dinuclear manganese(III) compounds involving similar bridging ligands, are collected in Table 4. Comparison of the structural properties of the ten compounds reveals four structural types with regard to the number of bridging alcoholate (or phenolate) oxygen atoms and the nature of the distortions and relative orientations of the manganese co-ordination octahedra. In the first structural type [Fig. 4(*a*)], illustrated by $[Mn^{III}_2(5Cl\text{-}salpro)_2(MeOH)]$,[4] $[Mn^{III}_2(salpro)_2(thf)]$,[5] $[Mn^{III}_2(salpro)_2(H_2O)]\cdot 3MeOH$[21] and **3**, one alcoholate oxygen atom bridges the two manganese cations separated by 3.76–3.82 Å. The individual z axes in these molecules are oriented at an angle close to 130°, and superexchange proceeds formally from the d_{z^2} orbital of one manganese to the $d_{x^2-y^2}$ orbital of the other. Since the $d_{x^2-y^2}$ orbital is unoccupied when D is negative, magnetic exchange interactions should be negligible for the d_{z^2}–$d_{x^2-y^2}$ pathway. However, the manganese environment is severely distorted from the idealized D_{4h} geometry, and mixing of the d_{z^2} and $d_{x^2-y^2}$ orbitals provides a plausible exchange mechanism for the weak antiferromagnetic interaction observed for the four complexes of this structural type.

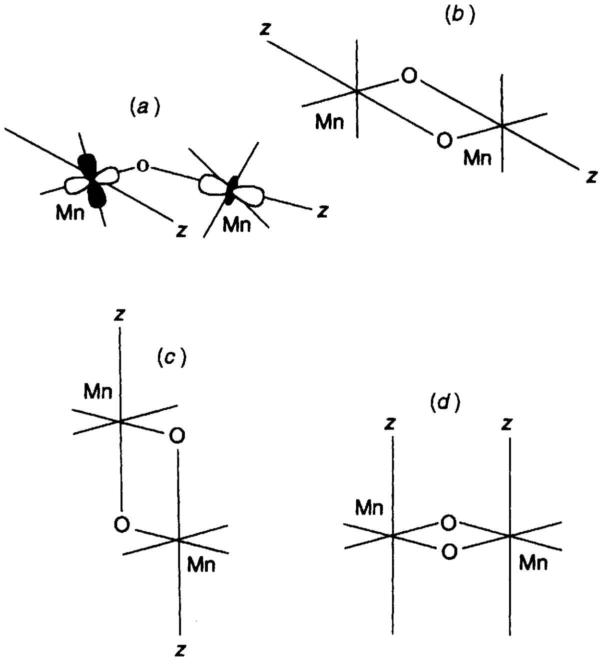

Fig. 4 Schematic representation of the manganese co-ordination octahedra and magnetic orbitals (*a*) for the four structural types in Table 4

In the second structural type [Fig. 4(*b*)], illustrated by $[\{Mn^{III}(5NO_2\text{-}salpro)\}_2]$[23] and **4**, two alcoholate oxygen anions bridge the two manganese cations separated by 3.23 and 3.22 Å, respectively. The individual z axes in these molecules are oriented at an angle close to 170°, and superexchange proceeds formally from the d_{z^2} orbital of one manganese to the $d_{x^2-y^2}$ orbital of the other manganese and *vice versa*. For the reasons mentioned in the previous paragraph, mixing of the d_{z^2} and $d_{x^2-y^2}$ orbitals provides a plausible exchange mechanism for the weak antiferromagnetic interaction observed for complex **4**. Further substantiation of this rationale could be gained from a study of the magnetic properties of $[\{Mn^{III}(5NO_2\text{-}salpro)\}_2]$.[23]

The main differences between the second [Fig. 4(*b*)] and third [Fig. 4(*c*)] structural types arise from a larger predominance of the axial elongation along z over all other distortions of the manganese co-ordination sphere in the structural type (*c*). This situation results from the fact that each manganese is chelated by all donor atoms of one ligand and the dinuclear unit results from dimerization of the resulting MnL molecules through either two alcoholate $\{[(Mn^{III}L)_2]\cdot 2Me_2CN$[24] ($H_3L$ = 1-salicylamino-3-salicylideneaminopropan-2-ol)} or phenolate $[\{Mn^{III}(3MeO\text{-}salen)Cl\}_2]$[33]

Table 4 Magnetostructural correlations for complexes **3** and **4** and dinuclear manganese(III) compounds having similar bridging ligands

Compound	Alcoholate bridges	Mn ··· Mn/Å	Mn–O–Mn/(°)	J/cm^{-1}	D/cm^{-1}	g_{xy}	g_{av}	g_z	Ref.
$[Mn^{III}_2(3NO_2\text{-salpro})_2(H_2O)]\cdot H_2O$ **3**	1			−1.93	−2.59	2.006		2.076	This work
$[Mn^{III}_2(5Cl\text{-salpro})_2(MeOH)]$	1	3.808(1)	128.9(2)	−3.55			1.95		4
$[Mn^{III}_2(\text{salpro})_2(\text{thf})]$	1	3.756(2)	124.5(1)	−5.50			2.00		5
$[Mn^{III}_2(\text{salpro})_2(H_2O)]$	1	3.818(3)	126.0(5)	−5.80			2.00		21
$[\{Mn^{III}(3NO_2\text{-salpro})\}_2]\cdot 2dmf$ **4**	2	3.223(1)	100.5(1)	−1.62	−2.51	2.041		2.098	This work
$[\{Mn^{III}(5NO_2\text{-salpro})\}_2]$	2	3.229(2)	99.9(1)						23
$[(Mn^{III}L)_2]\cdot 2MeCN$[a]	2	3.243(2)	100.7(3)	+4.50			2.00		24
$[\{Mn^{III}(3MeO\text{-salen})Cl\}_2]$	2[b]	3.572(5)	98.4(1)	+0.33	−0.96	1.980		2.105	33
$[Mn^{III}_2L'(OMe)Cl_2(MeOH)_2]$[c]	2	3.006(2)	101.6(2)	−15.6			2.01		34
$[Mn^{III}_2L'(OMe)(NCO)_2(H_2O)_2]$[c]	2	2.980(3)	100.3(5)	−16.5			2.00		34

[a] H_3L = 1-Salicylamino-3-salicylideneaminopropan-2-ol. [b] Phenolate bridges. [c] H_3L' = 1,5-Bis(salicylideneamino)pentan-3-ol.

Table 5 Electrochemical parameters obtained for complexes **3** and **4**

		Linear voltammetry[a]		Cyclic voltammetry[b]			
Complex	Solvent	$E_{\frac{1}{2}}$/mV	I_D/μA	E_{p_c}/mV	E_{p_a}/mV	$\frac{1}{2}(E_{p_c} + E_{p_a})$/mV	I_{p_c}/I_{p_a}
3	thf	114	−0.8	102	218	160	0.96
		612	0.4	636	695	666	1.08
	dmf	−313	−2.0	−176	225	25	0.95
		638	2.0	540	666	603	0.82
4	dmf	−322	−3.0	−133	206	37	0.96
		610	2.0	538	646	592	0.93
	dmf–water			−249	−59	−154	1.10
				166	240	203	0.65
				516	664	590	0.90

[a] Scan rate 5 mV s^{-1}, rotation speed 1000 revolutions min^{-1}. [b] Scan rate 100 mV s^{-1}.

{[H_2salen = *N,N'*-bis(salicylidene)ethane-1,2-diamine]} oxygen atoms. Since the manganese environment is close to the idealized D_{4h} geometry, mixing of the d_{z^2} and $d_{x^2-y^2}$ orbitals should be negligible and as the $d_{x^2-y^2}$ orbital is unoccupied when D is negative the magnetic exchange interactions should be negligible for the d_{z^2}–$d_{x^2-y^2}$ pathway. The weak ferromagnetic interaction observed for the two complexes of structural type (*c*) seems to confirm this interpretation while the difference in Mn ··· Mn distances between [$(Mn^{III}L)_2$]·2MeCN (3.24 Å) and [{Mn^{III}(3MeO-salen)Cl}$_2$] (3.57 Å) is reflected in the corresponding exchange integrals of 4.5 and 0.33 cm^{-1}, respectively.

In the fourth structural type [Fig. 4(*d*)] corresponding to the complexes [$Mn^{III}{}_2L'(OMe)Cl_2(MeOH)_2$] and [$Mn^{III}{}_2L'(OMe)(NCO)_2(H_2O)_2$][34] [$H_3L'$ = 1,5-bis(salicylideneamino)pentan-3-ol] the two bridging alcoholate oxygens are not situated on the individual *z* axes corresponding to axial elongation of the co-ordination octahedra and the Mn ··· Mn distances are shorter than in the other three structural types (≈3.0 Å). Consequently, the rationale considered in the previous paragraph indicates that no superexchange interaction can be transmitted through the d_{z^2}–$d_{x^2-y^2}$ pathway. However, the short Mn ··· Mn distance may allow direct overlap between the d_{xy} orbitals of the two manganese ions of each dinuclear unit, thus providing a plausible exchange mechanism for the ≈ −15 cm^{-1} antiferromagnetic interaction observed for the two complexes characterized by this type of structure. On the same grounds, it is interesting that exchange interactions of the same order of magnitude have been observed for manganese(III) complexes of structural types related to 4(*d*) in which one or two carboxylates afford additional bridges located at the apices corresponding to the *z* axes.[34,35]

Electrochemical Studies.—Complex **3** undergoes a one-electron quasi-reversible electrochemical oxidation close to 600 mV *vs.* saturated calomel electrode (SCE) in thf (Table 5). In this solvent, **3** retains a monoalkoxo-bridged structure similar to that of other [$Mn^{III}{}_2$(X-salpro)$_2$($O_{solvent}$)] complexes, as previously discussed (solvent = MeOH,[4] thf[5] or water[21]). On the other hand, as **4** results from the crystallisation of **3** in dmf, the dmf solutions of **3** and **4** are expected to have an electrochemical behaviour related to their dialkoxo-bridged structures. As confirmed by bulk electrolysis, despite this structural difference, **3** and **4** undergo a one-electron quasi-reversible electrochemical oxidation close to 600 mV *vs.* SCE in dmf (Table 5). However, the structural difference between **3** in thf and **3** and **4** in dmf clearly shows up on their reduction: while **3** undergoes a quasi-reversible electrochemical reduction close to 150 mV *vs.* SCE in thf, **3** and **4** undergo an irreversible electrochemical reduction close to 0 mV *vs.* SCE in dmf. The irreversibility is evidenced by the very large ΔE ($E_{p_a} - E_{p_c}$) values and the large discrepancies between the $E_{\frac{1}{2}}$ (linear voltammetry) and ($E_{p_a} + E_{p_c}$)/2 (cyclic voltammetry) values. Addition of one drop of water to the dmf solution of **4** results in the replacement of the irreversible reduction wave by two quasi-reversible reductions while there is no modification in the oxidation (Table 5). As confirmed by bulk electrolysis, the irreversible reduction of **3** and **4** in dmf is a two-electron process while the two quasi-reversible reductions of **4** in dmf–water are one-electron processes. Since the two bridging oxygen atoms of **3** and **4** are deprotonated, these results can be rationalized by considering that addition of a protic solvent allows formation of an intermediate $Mn^{II}Mn^{III}$ species in which the alcoholate function of one of the ligands is protonated. Further reduction of this dmf–water solution probably affords a $Mn^{II}{}_2$ species in which the alcoholate functions of both ligands are protonated.

The results described in this section indicate that the $Mn^{II}{}_2$, $Mn^{II}Mn^{III}$, $Mn^{III}{}_2$ and $Mn^{III}Mn^{IV}$ oxidation states are accessible for complex **4** in dmf–water. Although these results are in overall agreement with those described for dinuclear manganese(III) complexes with similar ligands, it should be underlined that the oxidation states accessible are $Mn^{II}{}_2$, $Mn^{III}{}_2$ and $Mn^{III}Mn^{IV}$ in the case of salpro, 5Cl-salpro, 3,5Cl_2-salpro and 5NO_2-salpro.[22,23] Complex **4** is thus the first dinuclear species in this series for which the redox equilibria involve all combinations of oxidation states.

Conclusion

The present work clearly shows the variety of structural types and nuclearities obtained for manganese complexes including pentadentate Schiff bases of the X-H_3salpro series. In this regard, the central alcoholic function of such ligands plays a prominent role and synthetic strategies based on the control of its protonation state can be devised to govern the nature of the resulting manganese complexes. Thus, complex **2**, resulting from the reaction of manganese(II) acetate with the sodium salt of 3NO_2-salpro, is the first reported manganese(II) compound characterized by the Mn_2L stoichiometry with a ligand of this series. On the other hand, **1**, resulting from the reaction of manganese(II) acetate with 3NO_2-H_3salpro is characterized by the MnL stoichiometry. Two structurally different dinuclear manganese(III) complexes characterized by the same overall formulation [{Mn^{III}(3NO_2-salpro)(solvent)}$_2$] can be obtained from the reaction of **1** with O_2, according to the co-ordinating ability of the solvent. In non-dehydrated methanol, the oxygen atom of one water molecule is co-ordinated to one of the manganese cations affording an asymmetric dinuclear species [$Mn^{III}{}_2$(3NO_2-salpro)$_2$(H_2O)]·H_2O **3** in which one 3NO_2-salpro pentadentate trianion bridges the two manganese cations through its central alcoholate oxygen and distributes its four remaining donors symmetrically between both manganese cations. The other 3NO_2-salpro trianion distributes its five donor atoms asymmetrically (O^-N /and O^-NO^-) between the two manganese cations. When **3** is dissolved in dry dmf the water molecule is driven out of the manganese co-ordination sphere and a subsequent ligand environment reorganization affords [{$Mn^{III}(3NO_2$-salpro)}$_2$]·2dmf **4** in which the manganese(III) cations are bridged by the alcoholate anions of both $3NO_2$-salpro pentadentate trianions which distribute their four remaining donors symmetrically between the two cations.

The preparation of complex **3** from the reaction of **1** with dioxygen not only involves the oxidation of two Mn^{II} to Mn^{III}, but also deprotonation of the central alcoholic function of two $3NO_2$-Hsalpro ligands. The spontaneous deprotonation of the central alcoholic function of $3NO_2$-Hsalpro during the course of the manganese oxidation reaction is noteworthy because it usually requires a highly basic medium, as shown by the reactions carried out for the preparation of the manganese(II) species. Association of the oxidation and deprotonation reactions (1) and (2) can be suggested to account for the overall reaction (3).

$$2Mn^{2+} + O_2 \longrightarrow 2Mn^{3+} + O_2{}^{2-} \quad (1)$$

$$2\text{Hsalpro}^{2-} + O_2{}^{2-} \longrightarrow 2\text{salpro}^{3-} + H_2O_2 \quad (2)$$

$$2Mn^{II}(\text{Hsalpro}) + O_2 \longrightarrow \{Mn^{III}(\text{salpro})\}_2 + H_2O_2 \quad (3)$$

Experimental

General.—Commercially available reagents and starting materials were used without further purification. Solvents were distilled under nitrogen and degassed under vacuum prior to use. Element analyses were carried out at the microanalytical laboratory of the Laboratoire de Chimie de Coordination for C, H and N, and at the Service Central de Microanalyses du CNRS in Vernaison for Mn. Infrared spectra were recorded on a Perkin-Elmer 983 spectrophotometer coupled with a Perkin-Elmer infrared data station. Samples were run as CsBr pellets prepared under nitrogen in a dry-box. Variable-temperature magnetic susceptibility data were obtained on powdered polycrystalline samples with a Quantum Design MPMS SQUID susceptometer. Diamagnetic corrections were applied by using Pascal's constants. Least-squares computer fittings of the data were accomplished with an adapted version of the function-minimization program STEPT.[36] X-Band powder and dmf–toluene glass ESR spectra were obtained on a Bruker ESP 300 E spectrometer with magnetic field modulation at 100 kHz. The microwave frequencies were measured with a Racal-Dana frequency meter and the magntic field was measured with a Bruker NMR probe gaussmeter. A Bruker liquid-nitrogen cryostat was used for measurements up to 90 K. Powdered and solution samples were loaded in 3 mm cylindrical quartz tubes in a dry-box, then degassed and sealed under vacuum. Cyclic voltammograms were obtained with a three-electrode cell comprised of a platinum working electrode, a platinum-wire counter electrode and a SCE reference electrode. Linear voltammograms were performed with a platinum rotating disc.

The compound $3NO_2$-H_3salpro was prepared following the method previously described for ligands of the same type.[10]

Complexes.—Complexes **1** and **2** were prepared under an atmosphere of purified nitrogen by using standard Schlenk techniques, isolated and stored in an inert-atmosphere box (Vacuum Atmospheres H.E.43.2) equipped with a Dri-Train (Jahan EVAC 7).

[$Mn^{II}_2(3NO_2$-salpro)(O_2CMe)]·4MeOH **2**. Manganese(II) acetate tetrahydrate (490 mg, 2 mmol) in methanol (10 cm^3) was added to a suspension of $Na_3(3NO_2$-salpro) (388 mg, 1 mmol) prepared by reaction of $3NO_2$-H_3salpro with sodium methanolate (162 mg, 3 mmol) in methanol (15 cm^3). The suspension dissolved and an orange precipitate formed progressively. The reaction mixture was stirred for 15 h at room temperature. After filtration, the orange complex **2** was washed with methanol and dried *in vacuo* (423 mg, 62%) (Found: C, 40.7; H, 4.7; Mn, 16.3; N, 8.4. $C_{23}H_{32}Mn_2N_4O_{13}$ requires C, 40.5; H, 4.7; Mn, 16.1; N, 8.2%).

[$Mn^{II}(3NO_2$-Hsalpro)] **1** *and* [$Mn^{III}_2(3NO_2$-salpro)$_2$(H_2O)]·H_2O **3**. Manganese(II) acetate tetrahydrate (245 mg, 1 mmol) in methanol (10 cm^3) was added to a suspension of $3NO_2$-H_3salpro (388 mg, 1 mmol) in methanol (15 cm^3). The mixture was heated under reflux (20 h) with stirring. After filtration, the orange complex [$Mn^{II}(3NO_2$-Hsalpro)] **1** was washed with methanol and dried *in vacuo* (88 mg, 20%) (Found: C, 46.8; H, 3.1; Mn, 12.7; N, 12.2. $C_{17}H_{14}MnN_4O_7$ requires C, 46.3; H, 3.2; Mn, 12.5; N, 12.7%). Brown microcrystals of complex **3** formed in the filtrate upon standing in the air for several days. These were collected, washed with methanol and dried *in vacuo* (Found: C, 44.7; H, 3.2; Mn, 11.7; N, 12.0. $C_{34}H_{30}Mn_2N_4O_{16}$ requires C, 44.6; H, 3.3; Mn, 12.0; N, 12.2%).

[{$Mn^{III}(3NO_2$-salpro)}$_2$]·2dmf **4**. Dark brown crystals of complex **4** suitable for X-ray measurements were grown from **3** by recrystallization from dimethylformamide–toluene (1 : 1).

Crystal Structure Determination of [{$Mn^{III}(3NO_2$-salpro)}$_2$]·2dmf **4**.—*Crystal data.* $C_{40}H_{40}Mn_2N_{10}O_{16}$, $M = 1026.7$, triclinic, space group $P\bar{1}$, $a = 10.934(3)$, $b = 11.147(3)$, $c = 9.652(2)$ Å, $\alpha = 92.99(2)$, $\beta = 100.93(2)$, $\gamma = 71.44(2)°$, $U = 1094.9(5)$ Å^3 (by least-squares analysis of 25 automatically centred reflections, $\lambda = 0.710\,73$ Å), $Z = 1$, $D_c = 1.557$ g cm^{-3}, $F(000) = 528$. Dark brown parallelepiped, crystal dimensions 0.4 × 0.3 × 0.2 mm, μ(Mo-Kα) 6.3 cm^{-1}.

Data collection and processing. CAD4 diffractometer, ω–2θ mode with ω scan width = 0.80 + 0.35 tan θ, ω-scan speed = 1.65–8.24° min^{-1}, graphite-monochromated Mo-Kα radiation; 3837 reflections measured ($0 \leqslant \theta \leqslant 25°$, h − 13 to 13, k − 13 to 13, l 0–11), 2849 used with $I > 3\sigma(I)$ after empirical absorption corrections[37] (maximum, minimum transmission factors = 0.999, 0.913).

Structure analysis and refinement. The structure was solved by direct methods and refined by full-matrix least squares. All non-hydrogen atoms were refined anisotropically. The oxygen atoms of the nitro group bonded to C(16) were disordered. Their site occupancy factors were refined, and the final model included two orientations with 50% occupancy and distances constraints for O(61), O(71), O(62) and O(72). Hydrogen atoms were found in a Fourier difference synthesis and were included in calculations with a constrained geometry [d(C–H) = 0.97 Å]. Isotropic thermal parameters for H atoms were first allowed to vary and then kept fixed to $U_{iso} = 0.06$ Å^2 for those of [{$Mn^{III}(3NO_2$-salpro)}$_2$] and $U_{iso} = 0.1$ Å^2 for those of dmf. The atomic scattering factors and anomalous dispersion terms were taken from ref. 38. The final full-matrix least-squares refinement converged to $R = (\Sigma||F_o| - |F_c||/\Sigma|F_o|)$ and $R' = [\Sigma w(|F_o| - |F_c|)^2/(\Sigma w|F_o|)^2]^{\frac{1}{2}}$ values of 0.041 and 0.041 with $w = 1$. The goodness of fit was $s = 0.797$ with 2849 observations and 325 variable parameters. All calculations were performed on a Micro VAX 3400 computer using the programs MOLEN,[39] SHELXS 86,[40] SHELX 76[41] and ORTEP.[25]

Additional material available from the Cambridge Crystallographic Data Centre comprises H-atom co-ordinates, thermal parameters and remaining bond lengths and angles.

Acknowledgements

Z.-Y. Z. thanks the French Ministère des Affaires Etrangeres and the Société de Secours des Amis des Sciences for a doctoral fellowship.

References

1 J. N. R. Ruddick and J. R. Sams, *J. Organomet. Chem.*, 1973, **60**, 233.

2 J. H. Cameron and J. A. McEwan, *Inorg. Chim. Acta*, 1993, **211**, 111.

3 R. J. Butcher, G. Diven, G. Erickson, G. M. Mockler and E. Sinn, *Inorg. Chim. Acta*, 1986, **111**, L55.

4 J. A. Bonadies, M. L. Kirk, M. S. Lah, D. P. Kessissoglou, W. E. Hatfield and V. L. Pecoraro, *Inorg. Chem.*, 1989, **28**, 2037.

5 K. Bertoncello, G. D. Fallon, K. S. Murray and E. R. T. Tiekink, *Inorg. Chem.*, 1991, **30**, 3562.

6 F. Tisato, F. Refosco, U. Mazzi, G. Bandoli and A. Dolmella, *Inorg. Chim. Acta*, 1989, **164**, 127.

7 V. V Zelentsov, I. K. Somova, R. S. Kurtanidze and T. B. Nikolaeva, *Koord. Khim.*, 1980, **6**, 1576.

8 J. P. Tuchagues and D. N. Hendrickson, *Inorg. Chem.*, 1983, **22**, 2545.

9 G. D. Fallon, A. Markiewicz, K. S. Murray and T. Quach, *J. Chem. Soc., Chem. Commun.*, 1991, 198.

10 B. Mabad, P. Cassoux, J. P. Tuchagues and D. N. Hendrickson, *Inorg. Chem.*, 1986, **25**, 1420.

11 W. Mazurek, K. J. Berry, K. S. Murray, M. J. O'Connor, M. R. Snow and A. G. Wedd, *Inorg. Chem.*, 1982, **21**, 3071.

12 Y. Nishida, M. Takeuchi, K. Takahashi and S. Kida, *Chem. Lett.*, 1985, 631.

13 M. Mazurek, B. J. Kennedy, K. S. Murray, M. J. O'Connor, J. R. Rodgers, M. R. Snow, A. G. Wedd and P. R. Zwack, *Inorg. Chem.*, 1985, **24**, 3258.

14 Y. Nishida and S. Kida, *J. Chem. Soc., Dalton Trans.*, 1986, 2633.

15 M. Mazurek, A. M. Bond, M. J. O'Connor and A. G. Wedd, *Inorg. Chem.*, 1986, **25**, 906.

16 Y. Nishida and S. Kida, *Inorg. Chem.*, 1988, **27**, 447.

17 J. C. Dutton, K. S. Murray and E. R. T. Tiekink, *Inorg. Chim. Acta*, 1989, **166**, 5.

18 K. Wieghardt, *Angew. Chem., Int. Ed. Engl.*, 1989, **28**, 1153.

19 L. Que, Jun. and A. E. True, *Prog. Inorg. Chem.*, 1990, **38**, 97.

20 J. E. Penner-Hahn, in *Manganese Redox Enzymes*, ed. V. L. Pecoraro, VCH, New York, 1992, p. 29.

21 M. Mikuriya, Y. Yamato and T. Tokii, *Bull. Chem. Soc. Jpn.*, 1992, **65**, 1466.

22 E. Larson, A. Haddy, M. L. Kirk, R. H. Sands, W. E. Hatfield and V. L. Pecoraro, *J. Am. Chem. Soc.*, 1992, **114**, 6263.

23 A. Gelasco and V. L. Pecoraro, *J. Am. Chem. Soc.*, 1993, **115**, 7928.

24 M. Mikuriya, Y. Yamato and T. Tokii, *Chem. Lett.*, 1992, 1571.

25 C. K. Johnson, ORTEP, Report ORNL-1794, Oak Ridge National Laboratory, Oak Ridge, TN, 1965.

26 G. B. Deacon and R. J. Phillips, *Coord. Chem. Rev.*, 1980, **33**, 227.

27 K. Nakamoto, *Infrared Spectra of Inorganic and Coordination Compounds*, 4th edn., Wiley, New York, 1986.

28 J. R. Ferraro, *Low Frequency Vibrations of Inorganic and Coordination Compounds*, Plenum, New York, 1971.

29 R. D. Dowsing, J. F. Gibson, D. M. Goodgame, M. Goodgame and P. J. Hayward, *Nature (London)*, 1968, **219**, 1037; R. D. Dowsing, J. F. Gibson, M. Goodgame and P. J. Hayward, *J. Chem. Soc. A*, 1969, 187; R. D. Dowsing, J. F. Gibson, D. M. Goodgame, M. Goodgame and P. J. Hayward, *J. Chem. Soc. A*, 1969, 1242; A. Abragam and B. Bleaney, *Résonance Paramagnétique Electronique des Ions de Transition*, Presses Universitaires de France, Paris, 1971; B. A. Goodman and J. B. Raynor, *Adv. Inorg. Chem. Radiochem.*, 1970, **13**.

30 C. J. O'Connor, *Prog. Inorg. Chem.*, 1982, **29**, 203.

31 A. P. Ginsberg and M. E. Lines, *Inorg. Chem.*, 1972, **11**, 2289.

32 P. Garge, R. Chikate, S. Padhye, J. M. Savariault, P. De Loth and J. P. Tuchagues, *Inorg. Chem.*, 1990, **29**, 3315 and refs. therein.

33 B. Mabad, D. Luneau, S. Theil, F. Dahan, J. M. Savariault and J. P. Tuchagues, 5th International Conference on Bioinorgic Chemistry, Oxford, 4–10th August, 1991; *J. Inorg. Biochem.*, 1991, **43**, 373; S. Theil, Ph.D. Thesis, Toulouse III University, 1993.

34 M. Mikuriya, Y. Yamato and T. Tokii, *Chem. Lett.*, 1991, 1429; *Inorg. Chim. Acta*, 1991, **181**, 1; *Bull. Chem. Soc. Jpn.*, 1992, **65**, 2624.

35 N. Torihara, M. Mikuriya, H. Okawa and S. Kida, *Bull. Chem. Soc. Jpn.*, 1980, **53**, 1610; M. Mikuriya, N. Torihara, H. Okawa and S. Kida, *Bull. Chem. Soc. Jpn.*, 1981, **54**, 1063; Y. Nishida, N. Oshino and T. Tokii, *Z. Naturforsch., Teil* B, 1988, **43**, 472; M. Mikuriya, S. Kida and I. Murase, *Chem. Lett.*, 1988, 35.

36 J. P. Chandler, Program 66, Quantum Chemistry Program Exchange, Indiana University, 1973.

37 A. C. T. North, D. C. Phillips and F. S. Mathews, *Acta. Crystallogr., Sect. A*, 1968, **24**, 351.

38 *International Tables for X-Ray Crystallography*, Kynoch Press, Birmingham, 1974, vol. 4.

39 C. K. Fair, MOLEN, Structure Solution Procedures; Enraf-Nonius: Delft, 1990.

40 G. M. Sheldrick, SHELXS 86, Program for Crystal Structure Solution; University of Göttingen, 1986.

41 G. M. Sheldrick, SHELX 76, Program for Crystal Structure Determination; University of Cambridge, 1976.

Received 27th October 1994; *Paper* 4/06583B